Available online at www.sciencedirect.com
ScienceDirect
Atmospheric Environment 42 (2008) 5760–5770
ATMOSPHERIC ENVIRONMENT
www.elsevier.com/locate/atmosenv

A comparison of CMAQ HONO predictions with observations from the Northeast Oxidant and Particle Study

Golam Sarwar[a,*], Shawn J. Roselle[b,1], Rohit Mathur[b,1], Wyat Appel[b,1], Robin L. Dennis[b,1], Bernhard Vogel[c]

[a]*National Exposure Research Laboratory, US Environmental Protection Agency, RTP, NC 27711, USA*
[b]*Atmospheric Sciences Modeling Division, Air Resources Laboratory, National Oceanic and Atmospheric Administration, RTP, NC 27711, USA*
[c]*Institut fur Meteorologie und Klimaforschung, Forschungszentrum Karlsruhe/Universitaet Karlsruhe, Postfach 3640, Karlsruhe D-76021, Germany*

Received 20 July 2007; received in revised form 26 December 2007; accepted 26 December 2007

Abstract

Predictions of nitrous acid from the Community Multiscale Air Quality modeling system are compared with the measurements from the 2001 Northeast Oxidant and Particle Study. Four different sources of nitrous acid were considered in the study: gas-phase reactions, direct emissions, a heterogeneous reaction, and a surface photolysis reaction. When only gas-phase reactions were considered in the model, the diurnally averaged mean bias, the normalized mean bias, the root mean square error, and the normalized mean error of the model were −1.01 ppbv, −98%, 1.05 ppbv, and 98%, respectively. However, the diurnally averaged mean bias, normalized mean bias, the root mean square error, and the normalized mean error of the model improved to −0.42 ppbv, −41%, 0.45 ppbv, and 41%, respectively, when all sources were considered. Model results suggest that the heterogeneous reaction and the surface photolysis reaction are the most important sources of nitrous acid in the atmosphere, accounting for about 86% of the predicted nitrous acid. Emissions and the gas-phase reactions were relatively minor sources and accounted for only 14% of the predicted nitrous acid. Model predictions suggest that the heterogeneous reaction is the most significant source of nitrous acid at night, while the surface photolysis reaction is the most significant source during the day. The addition of these sources increased the diurnally averaged hydroxyl radicals and ozone by 10% and 1.4 ppbv, respectively.
Published by Elsevier Ltd.

Keywords: Nitrous acid; Homogeneous reaction; Heterogeneous reaction; Surface photolysis reaction; Emissions

1. Introduction

Since the first identification of nitrous acid (HONO) in the atmosphere (Perner and Platt, 1979), its presence has been observed in many urban and rural environments (Harris et al., 1982; Lammel and Perner, 1988; Appel et al., 1990; Vecera and Dasgupta, 1991; Febo et al., 1993; Winer and

*Corresponding author. Tel.: +1 919 541 2669; fax: +1 919 541 1379.
E-mail address: sarwar.golam@epa.gov (G. Sarwar).
[1]In Partnership with National Exposure Research Laboratory, US Environmental Protection Agency, RTP, NC 27711, USA.

1352-2310/$ - see front matter Published by Elsevier Ltd.
doi:10.1016/j.atmosenv.2007.12.065

Biermann, 1994; Zhou et al., 2002). For example, Vecera and Dasgupta (1991) measured HONO mixing ratios in Lubbock, Texas, and reported that the nighttime mixing ratios ranged between 1.0 and 2.0 parts per billion by volume (ppbv), while the daytime mixing ratios ranged between 100 and 500 parts per trillion by volume (pptv). Febo et al. (1993) measured HONO mixing ratios of up to 10 ppbv in Milan, Italy. Winer and Biermann (1994) measured HONO mixing ratios of up to 15 ppbv in southern California. Zhou et al. (2002) performed ambient measurements at a rural site in New York and reported a daytime HONO mixing ratio of 60 pptv. Most studies suggest that the observed HONO mixing ratios are greater at night than during the day.

The importance of HONO chemistry in producing hydroxyl radical (OH) is well known (Winer and Biermann, 1994; Harrison et al., 1996; Alicke et al., 2002, 2003; Acker et al., 2006). Winer and Biermann (1994) reported that the photolysis of HONO was responsible for the large OH formation rate in the early morning hours in southern California. Alicke et al. (2002) measured ambient HONO and other chemical species in Milan, Italy, and suggested that the photolysis of HONO was the most significant source of OH during the first 4–6 h after the sunrise. On a daily basis, the photolysis of HONO contributed up to 34% of total OH formation. Alicke et al. (2003) measured ambient HONO near Berlin, Germany, and also suggested that the photolysis of HONO was the most significant source of OH in the early morning hours. The photolysis of HONO provided as much as 20% of daily integrated OH. Acker et al. (2006) measured HONO at a rural site in Germany during summer 2002 and 2004 and reported that the photolysis of HONO produced 42% of the integrated photolytic HO_x ($OH + HO_2$) formation (HO_2 = hydroperoxy radical).

While the effect of HONO on OH is well known, the chemical reactions producing HONO are not well understood. Most air quality models employ only homogeneous chemical reactions for HONO. For example, the most updated Carbon Bond (CB05) chemical mechanism contains five homogeneous reactions related to HONO (Yarwood et al., 2005):

$$NO + NO_2 + H_2O \rightarrow 2.0HONO, \quad k = 5.0 \times 10^{-40}, \tag{1}$$

$$NO + OH \rightarrow HONO,$$
$$k = \left\{\frac{k_0[M]}{(1 + k_0[M]/k_1)}\right\} 0.6^{\{1+[\log_{10}(k_0[M]/k_1)]^2\}^{-1}}, \tag{2}$$

$$k_0 = 7.0 \times 10^{-31}\left(\frac{T}{300}\right)^{-2.6},$$

$$k_1 = 3.6 \times 10^{-11}\left(\frac{T}{300}\right)^{-0.1},$$

$$HONO + h\gamma \rightarrow NO + OH, \quad J = 0.002\,s^{-1}, \tag{3}$$

$$OH + HONO \rightarrow NO_2 + H_2O,$$
$$k = 1.8 \times 10^{-11} e^{(-390/T)}, \tag{4}$$

$$HONO + HONO \rightarrow NO + NO_2 + H_2O,$$
$$k = 1.0 \times 10^{-20}, \tag{5}$$

where NO is nitric oxide, NO_2 is nitrogen dioxide, H_2O is water vapor, k is the expression for a rate constant, T the temperature in K, M the total pressure in molecules cm^{-3}, and J the photolysis rate at a latitude of 40°N (typical summer noon). Chemical reactions in other widely used atmospheric chemical mechanisms are also similar. For example, the Carbon Bond IV (CB-IV) mechanism also contains the same five chemical reactions for HONO (Gery et al., 1989). The Statewide Air Pollution Research Center (SAPRC-99) mechanism contains four chemical reactions for HONO (Carter, 2000).

Several studies have indicated that the following heterogeneous reactions can play a significant role in HONO chemistry (Svensson et al., 1987; Calvert et al., 1994; Ammann et al., 1998; Kleffmann et al., 1998; Aumont et al., 2003):

$$NO + NO_2 + H_2O \rightarrow 2HONO, \tag{6}$$

$$NO_2 + \text{aerosol surface} \rightarrow HONO + \text{oxidized aerosol surface}, \tag{7}$$

$$2NO_2 + H_2O \rightarrow HONO + HNO_3, \tag{8}$$

where NO is nitric oxide and HNO_3 is nitric acid. The heterogeneous reaction involving NO, NO_2, and H_2O (reaction (6)) has been studied extensively; its reported rate constant is quite uncertain and varies by two orders of magnitude based on current literature (Cai, 2005 and the references therein). However, Kleffmann et al. (1998) suggest that it is not a significant contributor to HONO. Ammann et al. (1998) suggest that the reaction of NO_2 on

a fresh soot surface can produce HONO in the atmosphere (reaction (7)); however, the recent studies indicate that it may not be an important pathway for HONO production in the atmosphere since surface deactivation occurs within a few minutes (Kleffmann et al., 1999; Arens et al., 2001).

Recent studies also suggest the possibility of the production of HONO via surface photolysis (Zhou et al., 2001, 2002, 2003; Vogel et al., 2003; Acker et al., 2006). Zhou et al. (2001) performed laboratory experiments and ambient measurements at a special trailer site in Alert, Canada, and indicated that a significant formation of HONO occurs via photochemical production in the snowpack. Zhou et al. (2002) suggested the existence of a strong daytime HONO source and proposed that the photolysis of adsorbed HNO_3 produces the daytime HONO. Acker et al. (2006) reported elevated daytime HONO mixing ratios and also suggested the existence of an unknown daytime HONO source in the atmosphere.

Studies have indicated that air quality models that take into account only the homogeneous reactions are not adequate to explain the observed ambient HONO mixing ratios (Moussiopoulos et al., 2000; Vogel et al., 2003). Moussiopoulos et al. (2000) used a multilayer photochemical dispersion model to investigate the role of heterogeneous sources on HONO. They applied the model to simulate HONO in Milan, Italy, and concluded that heterogeneous reactions were primarily responsible for producing HONO; homogeneous reactions did not contribute significantly. Vogel et al. (2003) used a one-dimensional model to study the relative importance of various HONO sources. They applied the model to simulate air quality at a site in Germany and indicated that direct emissions and heterogeneous reactions were the most important sources of HONO at night. The predicted HONO mixing ratios were lower than the observed data during the day. When they added an artificial photolytic source of HONO to the model, the predicted HONO mixing ratios increased during the day and agreed with the observed data. The use of three-dimensional air quality models to study HONO chemistry is limited. The objective of this study is to use a three-dimensional air quality model to evaluate the model performances for HONO by comparing the model predictions with measurements from the Northeast Oxidant and Particle Study (NEOPS) and to assess the relative importance of four different HONO sources: direct emissions, homogeneous reactions, heterogeneous reactions, and surface photolysis.

2. Methodology

Model simulations were performed using the Community Multiscale Air Quality (CMAQ) modeling system (version 4.6; Binkowski and Roselle, 2003; Byun and Schere, 2006). The modeling domain consisted of 124×108 horizontal grid cells over the eastern United States with 12-km grid spacings and 14 vertical layers of variable thickness between the surface and 100 mb (Fig. 1). The CMAQ chemical transport model was configured to use the mass continuity scheme to describe advection processes, the Asymmetric Convective model version 2 (ACM2) (Pleim, 2007) to describe vertical diffusion processes, the multiscale method to describe horizontal diffusion processes, and an adaptation of the ACM algorithm for convective cloud mixing. Aqueous chemistry, aerosol processes, and dry and wet deposition were also included. The meteorological driver for the CMAQ modeling system was the PSU/NCAR MM5 system (version 3.5; Grell et al., 1994). Initial and boundary conditions for this study were obtained from a larger modeling domain consisting of 148×112 grid cells with a 36-km grid spacing for the continental United States. Model simulations were performed using the CB05 mechanism for 1–30 July 2001 with a spin-up period of 7 days.

The 1999 National Emissions Inventory (version 3) grown to 2001 was used to generate model-ready emissions using the Sparse Matrix Operator Kernel Emission (SMOKE) (Houyoux et al., 2000). The Biogenic Emissions Inventory system (version 3.13)

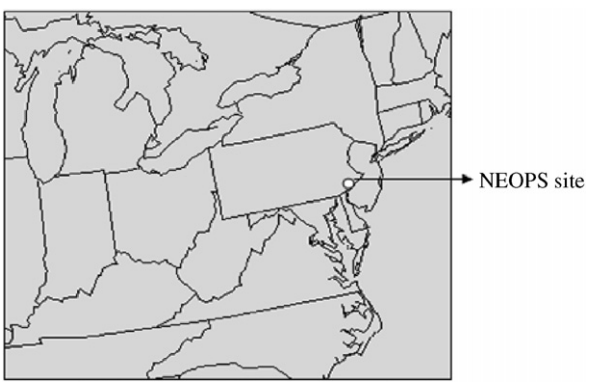

Fig. 1. Modeling domain used in the study.

was used to prepare biogenic emissions for the study (Schwede et al., 2005).

2.1. Direct emissions

Thermodynamics and kinetics are not conducive for HONO formation in combustion systems (Calvert et al., 1994). However, HONO can form in combustion systems as the temperature of the combustion products is decreased. Measurements of HONO emissions from combustion systems are somewhat limited. Most studies have focused on the measurements of HONO emissions from motor vehicles. Only a few studies focused on HONO emissions from other combustion sources. For example, Wormhoudt et al. (2007) measured oxides of nitrogen (NO_x) and HONO emissions in aircraft exhausts and reported that HONO emissions can range up to 7% of the NO_x emissions. HONO formations from indoor combustion sources (kitchen stoves, kerosene and propane space heaters, etc.) have also been measured (Pitts et al., 1989; Brauer et al., 1990).

Several studies have focused on HONO emissions from motor vehicles. For example, Kessler and Platt (1984) reported an emissions ratio of 0.01 for $HONO/NO_x$ for a diesel engine. They also reported an emissions ratio of <0.0001 and 0.0015 for $HONO/NO_x$ for a gasoline engine at a fuel-rich and fuel-lean operating condition, respectively. Calvert et al. (1994) reported an emissions ratio of <0.001 for $HONO/NO_x$ for a catalyst-equipped gasoline engine vehicle. Kurtenbach et al. (2001) measured HONO and NO_x emissions from three vehicles: a diesel engine powered truck, a diesel engine powered passenger car, and a gasoline engine powered passenger car. They reported an emissions ratio of 0.008, 0.0066, and 0.0053 for $HONO/NO_x$ for the truck, the diesel engine powered car, and the gasoline engine powered car, respectively. Since emissions of individual vehicle depend on engine type and operating conditions, an alternative approach has been used for estimating HONO emissions from on-road motor vehicles. In such approaches, ambient HONO, NO_x, and other appropriate parameters are measured in road tunnels in order to derive an estimate of HONO emissions. Kirchstetter and Littlejohn (1996) conducted such an experiment in the Caldecott tunnel in San Francisco, California, and reported a value of 2.9×10^{-3} for the $HONO/NO_x$ emissions ratio. Kurtenbach et al. (2001) conducted a similar study in the Wuppertal Kiesbergtunnel and reported a value of 8×10^{-3} for the same ratio. For this study, HONO emissions were estimated using a value of 8×10^{-3} for the $HONO/NO_x$ emissions ratio for on-road and off-road vehicles. HONO emissions are currently not used in the CMAQ modeling system.

2.2. Heterogeneous reactions

The heterogeneous reaction involving NO_2 and H_2O (reaction (8)) has been shown to be important for HONO production in the atmosphere (Svensson et al., 1987; Kleffmann et al., 1998; Vogel et al., 2003). Laboratory studies suggest that reaction (8) is first order in NO_2 (Finlayson-Pitts and Pitts, 2000) and can occur on aerosol and ground surfaces. Following Kurtenbach et al. (2001), this heterogeneous reaction is implemented into the CMAQ modeling system with a rate constant of $3.0 \times 10^{-3} S/V\,\mathrm{m}^{-1}$ (S/V is the ratio of surface area to volume of air). Aerosol surface areas are generally much smaller than ground surface areas; thus aerosol surface areas are less effective in producing HONO in the atmosphere via this heterogeneous reaction. However, the heterogeneous reaction on aerosol surfaces was also included in the model for completeness. Ground surface areas provided by leaves can be estimated using the leaf area index (LAI). Jones (2006) suggests that the use of LAI underestimates leaf surface areas by at least a factor of two since it accounts only for areas on one side of the leaves. Thus, the S/V ratios for leaves were estimated as follows:

$$S/V = 2\ \mathrm{LAI}/\text{surface layer height in the model.} \quad (9)$$

Buildings and other structures can also enhance ground surface areas in urban environments. However, estimates of these areas are not readily available. In the absence of such information, an ad hoc approach was used to estimate the ground surface areas for buildings and other structures in urban environments. Svensson et al. (1987) studied the kinetics of the reaction involving NO_2 and H_2O and suggested a value of $0.2\,\mathrm{m}^{-1}$ for typical urban environments. They, however, also indicated that some building materials may provide an order of magnitude greater surface area than their simple projected surface areas due to porosity and roughness. For this study, the S/V ratio for buildings and other structures at the grid cell with the highest urban environment was assigned a value of $0.3\,\mathrm{m}^{-1}$. The S/V ratios for buildings and other structures for

other urban environments were linearly scaled to this S/V ratio by assuming that the values are proportional to the percent urban area in any grid cell. Using this procedure, the total S/V ratio for the grid cell containing northeast Philadelphia was estimated to be $0.28\,m^{-1}$, which is much lower than the value of $1.3\,m^{-1}$ used by Cai (2005) for New York. HONO produced via the heterogeneous reaction on ground surfaces was released into the first layer of the model.

2.3. Surface photolysis

Zhou et al. (2003) recently conducted laboratory experiments and suggested that adsorbed HNO_3 on surfaces can undergo photolysis to produce HONO and NO_2. Adsorbed HONO and NO_2 are then released into the atmosphere via desorption. A simplified photolysis reaction producing HONO and NO_2 was added to the CMAQ modeling system (reaction (10)). Adsorbed HNO_3 on ground surfaces is assumed to equal the amount of HNO_3 accumulated over time by dry deposition since the last precipitation event. The model assumes that any precipitation event cleanses the adsorbed HNO_3; thus it is reset to zero following the precipitation event.

$$HNO_3(ads) \rightarrow 0.5HONO(ads) + 0.5NO_2(ads), \tag{10}$$

where HNO_3(ads) is adsorbed nitric acid, HONO(ads) is adsorbed nitrous acid, and NO_2(ads) is adsorbed nitrogen dioxide. The reaction can also produce adsorbed ground state oxygen atom and OH, which have been neglected in the study.

Zhou et al. (2003) reported a photolysis rate of $1.3 \times 10^{-3}\,min^{-1}$ at noontime tropical conditions for the surface photolysis of adsorbed nitric acid. The reported value is 24 times greater than the CMAQ-estimated photolysis rate of gaseous HNO_3 in the lowest layer of the model during summertime conditions (latitude 10°N). The surface photolysis rate of adsorbed HNO_3 was estimated as 24 times the photolysis rate of gaseous HNO_3 used in the CMAQ modeling system. HONO and NO_2 produced via the surface photolytic reaction was released into the first layer of the model.

2.4. Establishing the model to measurement comparisons

Model predictions were compared with measurements from the NEOPS between 1 July and 30 July 2001 in northeast Philadelphia (Philbrick et al., 2002). The measurement site was located at the City of Philadelphia's Baxter water treatment plant between the US Interstate 95 and the Delaware River (40°2.14′N 75°0.28′W, Fig. 1). The site can be characterized as an urban area and is situated about 13 km northeast of the city center. Ambient mixing ratios of HONO and other chemical species were continuously measured during the study. HONO mixing ratios were measured using an ion chromatography technique that has a detection limit in the sub-pptv range and an accuracy of about 5% (Simon and Dasgupta, 1995; Dasgupta, 2007). Measured data from the study were averaged on an hourly basis and used to calculate an average diurnal profile. The mean bias (MB), normal mean bias (NMB), root mean square error (RMSE), and the normal mean error (NME) of the model's average diurnal profiles were calculated using Eqs. (11)–(14) (Eder and Yu, 2006):

$$MB = \frac{1}{N}\sum_{1}^{N}(C_m - C_o), \tag{11}$$

$$NMB = \frac{\sum_1^N (C_m - C_o)}{\sum_1^N C_o}, \tag{12}$$

$$RMSE = \sqrt{\frac{1}{N}\sum_{1}^{N}(C_m - C_o)^2}, \tag{13}$$

$$NME = \frac{\sum_1^N |C_m - C_o|}{\sum_1^N C_o}, \tag{14}$$

where C_m is the average predicted diurnal profile, C_o the average observed diurnal profiles, and N the sample size.

The performance of the meteorological driver for CMAQ (MM5) proved to be within state-of-science capabilities. Gilliam et al. (2006) evaluated the MM5 model performances for summer 2001 by comparing the predicted meteorological fields with observed data from the National Center for Atmospheric Research. The MB, the mean absolute error (MAE), and the index of agreement (IA) for simulated 2-m air temperature for northeast US were 0.67 K, 2.43 K, and 0.93, respectively. The MB, the MAE, and the IA for predicted wind speed for the northeast US were $-0.12\,m\,s^{-1}$, $1.21\,m\,s^{-1}$, and 0.46, respectively. The MM5-predicted model performances at a specific northeast Philadelphia meteorological observation site were generally

better than those of the entire northeast US collectively. For example, the MB, the MAE, and the IA for predicted water mixing ratio at northeast Philadelphia were 0.31 g kg^{-1}, 1.61 g kg^{-1}, and 0.74, respectively. The MB, the MAE, and the IA for predicted air temperature at this site were 0.31 K, 1.50 K, and 0.92, respectively. The MB, the MAE, and the IA for predicted wind speed at the site were −0.28 m s^{-1}, 0.96 m s^{-1}, and 0.53, respectively. Air temperature and wind speed during the month ranged between 288 and 307 K, and 2 and 9 m s^{-1}, respectively. The mean air temperature in July 2001 was within 0.2 K of the 30-year average temperature (July) for the area. Meteorological conditions during the study period were generally representative of the summer season of the area.

Four different model simulations (cases A–D) were performed to assess the effects of various HONO sources on the predicted HONO. Case A used emissions that are typically used in the current CMAQ modeling system and the standard CB05 mechanism. Case B used HONO emissions along with emissions that were used in case A and the CB05 mechanism. Case C used emissions that were used in B, the CB05 mechanism, and the heterogeneous reaction (8). Case D used emissions that were used in C, the CB05 mechanism, the heterogeneous reaction (8), and the surface photolysis reaction (10).

3. Results and discussion

The model performances for ozone, aerosol sulfate, aerosol nitrate, ammonium, and fine particles ($PM_{2.5}$) are shown in Table 1 (case A). The mean predicted ozone was greater than the mean observed ozone; thus the model was biased positive. The MB for ozone was 2.6 ppbv, the NMB was 6.9%, the RMSE was 7.3 ppbv, and NME was 18%. The mean predicted aerosol sulfate was lower than the mean observed value by 0.2 μg m^{-3}. The MB for aerosol constituents ranged between −0.3 and 1.0 μg m^{-3}, the NMB between −13% and 19%, the RMSE between 0.3 and 2.5 μg m^{-3}, and the NME between 8.8% and 46%. With the exception of aerosol nitrate, the NMB and NME for each of the aerosol constituents were less than 13% and 20%, respectively. The overprediction of aerosol nitrate is caused by high values of the uptake coefficient for the heterogeneous reaction involving dinitrogen pentoxide and H_2O used in the model and was not the focus of the present study. With the exception of aerosol nitrate, the model was capable of reproducing the chemical species shown in Table 1 at the NEOPS site.

The mean observed HONO was 1.04 ppbv for the study period (Table 2). The mean predicted value for case A was about 35 times lower than the observed value. Thus, HONO was significantly underpredicted compared to the observed data. The MB and NMB for HONO were −1.01 ppbv and 98%, respectively. The RMSE and NME for HONO were 1.05 ppbv and 98%, respectively. While the MB for case A was similar to some of the chemical species shown in Table 1, the NMB and NME were much larger than for any chemical species shown in Table 1.

The average predicted and observed diurnal HONO mixing ratios are presented in Fig. 2. The observed HONO was greater at night than during the day and remained relatively constant from midnight to 7 am, then decreased from 7 am to 7 pm, then increased. The predicted HONO for case A from midnight to 6 am was only about 0.01 ppbv, then increased and peaked around noon, and then continuously decreased. The predicted HONO for

Table 1
Model performance statistics for selected chemical species at northeast Philadelphia (observed data are taken from NEOPS, model results for case A)

Species	Mean observed (ppbv or μg m^{-3})	Mean model (ppbv or μg m^{-3})	MB (ppbv or μg m^{-3})	NMB (%)	RMSE (ppbv or μg m^{-3})	NME (%)
Ozone	36.9	39.4	2.6	6.9	7.3	18
Aerosol sulfate	5.4	5.2	−0.2	−3.7	0.7	8.8
Aerosol nitrate	0.4	0.5	0.1	19	0.3	46
Ammonium	2.1	1.8	−0.3	−13	0.6	20
$PM_{2.5}$	11.8	12.8	1.0	8.1	2.5	18

Note: Unit of ozone in ppbv, units of aerosol sulfate, aerosol nitrate, ammonium, and $PM_{2.5}$ are in μg m^{-3}.

Table 2
Model performance statistics for HONO at northeast Philadelphia (observed data are taken from NEOPS)

Cases	Mean observed (ppbv)	Mean model (ppbv)	MB (ppbv)	NMB (%)	RMSE (ppbv)	NME (%)
A	1.04	0.03	−1.01	−98	1.05	98
B	1.04	0.08	−0.96	−92	0.99	92
C	1.04	0.46	−0.57	−55	0.60	55
D	1.04	0.62	−0.42	−41	0.45	41

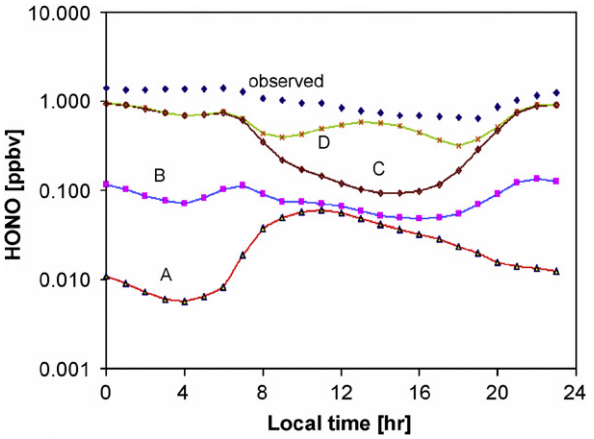

Fig. 2. A comparison of predicted diurnal HONO with observed data from the NEOPS. *Note*: log scale for HONO.

case A peaked during the day, while the observed data peaked at night. The average predicted and observed HONO mixing ratios during daytime and at night are also presented in Table 3. The maximum predicted HONO occurred during the day, while the maximum observed HONO occurred at night (Fig. 2 and Table 3). The average predicted HONO for case A was two orders of magnitude lower than the observed data at night and 21 times lower during the day. Contrary to the observed data, the predicted HONO mixing ratio for case A was greater during the day by a factor of four over the mixing ratio at night. Thus, the model failed to capture the magnitude and the diurnal variability of the observed data.

When HONO emissions were added to the model (case B), the predicted HONO mixing ratio increased at night, and was slightly higher than during the day. However, the predicted HONO mixing ratio was still lower than the observed data by a large margin both at night and during the day. The predicted HONO mixing ratio for case B during the day increased by only a small amount compared to case A, due to its high photolysis rate and higher mixing heights during the day. The average predicted HONO for case B was lower than the observed data by 12 times at night as well as during the day. The NMB and NME for case B improved to −92% and 92%, respectively.

When the heterogeneous reaction was also added to the model (case C), predicted HONO mixing ratios further increased. The mean predicted value improved to 0.46 ppbv. The average predicted night value reached to within 60% of the observed data at night. While the predicted HONO mixing ratios with case C during the day were greater than those with case B, the predicted values were still significantly lower than the observed data during the day. The average predicted daytime HONO mixing ratio was 4.2 times lower than the observed data. The MB, NMB, RMSE, and NME for case C improved to −0.57 ppbv, −55%, 0.60 ppbv, and 55%, respectively.

When the surface photolysis of adsorbed HNO_3 was also added to the model (case D), the predicted HONO mixing ratios increased during the day due to the increased HONO production. The mean predicted value improved to 0.62 ppbv. The average predicted daytime value reached to within 80% of the observed data. The MB, NMB, RMSE, and NME for case D improved to −0.42 ppbv, −41%, 0.45 ppbv, and 41%, respectively.

The relative contribution of these sources to predicted HONO is shown in Fig. 3. The heterogeneous reaction (Eq. (8)) was the largest contributor, representing, on average, 54% of the predicted HONO. It contributed up to 90% of the predicted HONO at night, while its contribution was much lower during the day. The surface photolysis reaction (Eq. (10)) was the second largest contributor and represented 32% of the predicted HONO. Its contribution peaked during the day. The average contribution of HONO emissions

Table 3
Comparison of predicted HONO with observed data from the NEOPS

Case	Night			Day		
	Observed HONO (ppbv)	Predicted HONO (ppbv)	Observed/ predicted (ratio)	Observed HONO (ppbv)	Predicted HONO (ppbv)	Observed/ predicted (ratio)
A	1.26	0.01	126	0.85	0.04	21
B	1.26	0.10	12	0.85	0.07	12
C	1.26	0.78	1.6	0.85	0.20	4.2
D	1.26	0.79	1.6	0.85	0.47	1.8

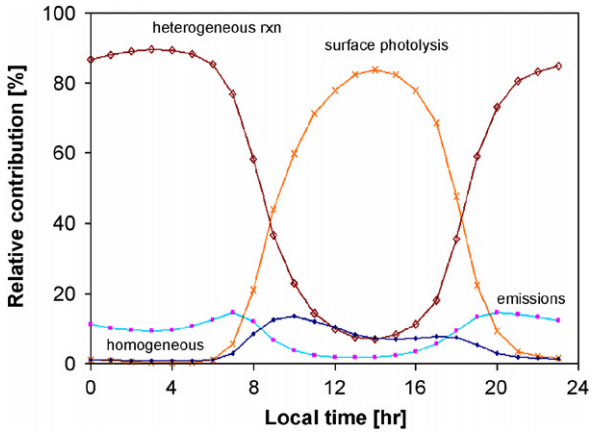

Fig. 3. Relative contribution of different sources to HONO at northeast Philadelphia (case D).

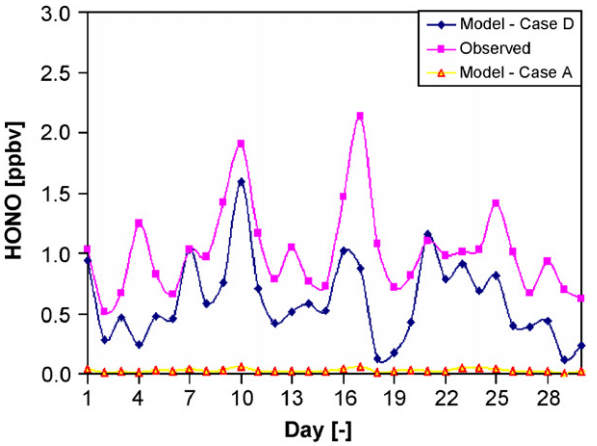

Fig. 4. Comparison of predicted daily averaged HONO with observed data from the NEOPS.

and homogeneous reactions were 9% and 5%, respectively.

The daily averaged HONO mixing ratios for cases A and D are compared to the observed data in Fig. 4. The observed HONO ranged from 0.52 to 2.2 ppbv. However, the predicted HONO for case A ranged only up to 0.06 ppbv. Predicted HONO mixing ratios for case A were 1–2 orders of magnitude lower than the observed data. The predicted HONO for case D ranged from 0.12 to 1.59 ppbv and were in better agreement with the observed data. The predicted HONO for case D was generally also lower than the observed data. Possible reasons that may have resulted in the lower HONO prediction for case D compared to the observed data include: (1) ground surface areas used in the study may need further refinement. As mentioned earlier, Jones (2006) suggests enhancing the LAI by at least a factor of two. A value of two was used in this study. Similarly, the S/V ratios for buildings and other structures for urban environments may also need further refinement; (2) Bejan et al. (2006) recently suggested that the photolysis of o-nitrophenol can also produce HONO in the atmosphere and stated that the production of HONO via such sources can explain, in part, daytime elevated observed HONO in the atmosphere. The current study does not include such sources; thus the predicted daytime HONO in the current study are likely to be lower than the observed values.

Aumont et al. (2003) used a two-layer box model to investigate sources of HONO. They used HONO emissions as well as a heterogeneous reaction on aerosols and the ground, and considered surface areas on aerosols and the ground for the heterogeneous reaction. They estimated the rate constant for the heterogeneous reaction on aerosol as $0.25\gamma cS$, where γ is the reactive uptake coefficient, c the mean molecular speed of NO_2, and S the aerosol surface area per volume of air. They estimated the rate constant for the heterogeneous reaction on ground surfaces as fv_d/h, where f is the

weighting factor for the conversion of NO_2 to HONO (a value of 0.5 was used), v_d the deposition velocity for NO_2, and h the mixing height. This approach was implemented into the CMAQ modeling system for purposes of comparison and simulations were performed for a 10-day period in July 2001. The average predicted HONO was lower than the observed data by a factor of two at night and seven during the day. Thus, our approach represents a significant improvement.

As mentioned above, HONO undergoes photolysis in the atmosphere to produce OH. The inclusion of additional HONO sources enhanced the diurnally averaged OH by only 10% with case D compared to that of case A. However, the predicted OH for case D increased by up to a factor of two during the morning hours compared to that with case A.

The impacts of additional HONO on ozone are presented in Fig. 5. Predicted ozone mixing ratios for case D increased by up to 2.4 ppbv compared to those of case A. The increases started during the morning hours and continued throughout the day. However, the increases in the ozone mixing ratios were not adequate to explain the observed early morning rise. The diurnally averaged ozone for case D increased by 1.4 ppbv compared to that of case A. The increased ozone is a contribution of additional oxidation of volatile organic compound via enhanced OH as well as the photolysis of additional NO_2 generated from the surface photolysis of adsorbed HNO_3.

The observed ratio of $HONO/HNO_3$ was 2.9 at night. For case A, the ratio was only 0.01 and increased to 0.3 for case D. During the day, the observed ratio was 0.73, compared to a value of only 0.02 for case A, which increased to 0.2 for case D.

4. Summary

Air quality simulations were performed using the CMAQ modeling system. The MB, NMB, RMSE, and NME for HONO predictions with only gas-phase production were poor. The inclusion of additional sources greatly improved the MB, NMB, RMSE, and NME for HONO. The results of this study suggest that heterogeneous reaction and surface photolysis of adsorbed HNO_3 are important sources of HONO in the atmosphere. Most air quality models, however, do not currently account for these sources; thus, models tend to significantly underpredict HONO. The implementation of the heterogeneous reaction into an air quality model requires the estimation of surface areas of leaves as well as surface areas of building and other structures in urban environments. Surface areas of leaves can be estimated using the LAI.

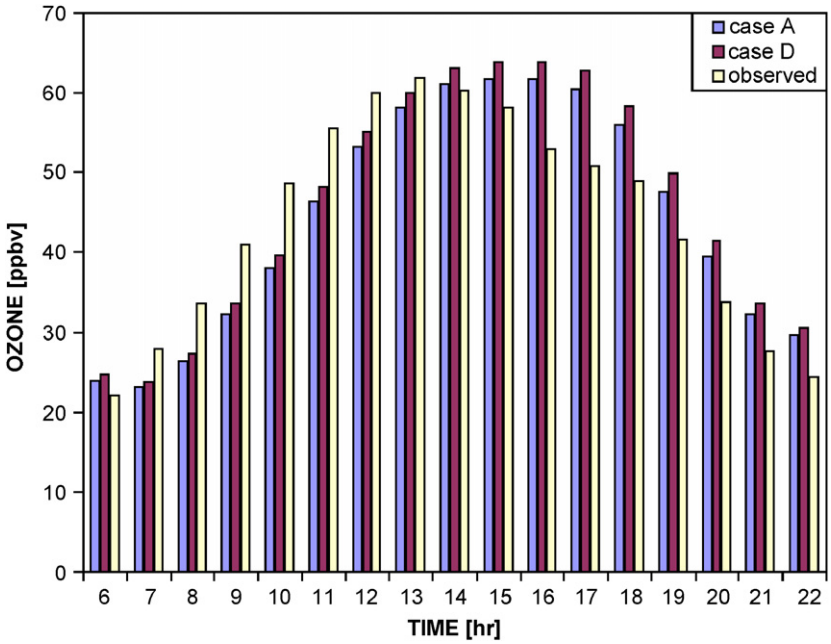

Fig. 5. Impact of additional HONO chemistry on ozone at northeast Philadelphia.

However, estimates of surface areas of buildings and other structures in urban environments are currently not readily available; efforts should be directed toward determining such values. The surface photolysis of adsorbed HNO_3 producing HONO and NO_2 during the day and the photolysis of other compounds is an emerging topic. Together with increased nighttime carry over due to improved surface area estimates, photolysis may help to provide the missing HONO source during the day, without which model predictions remain underpredicted compared to the observed data. Thus, these reactions should be further explored in the laboratory as well as field studies before they can be confidently used in air quality models.

Acknowledgments

Professor Purnendu K. Dasgupta of the University of Texas at Arlington and Professor C. Russell Philbrick of the Pennsylvania State University provided the observed data from the North East Oxidant and Particle Study.

Disclaimer: The research presented here was performed under the memorandum of understanding between the US Environmental Protection Agency (EPA) and the US Department of Commerce's National Oceanic and Atmospheric Administration (NOAA) and under Agreement DW13921548. This work constitutes a contribution to the NOAA Air Quality Program. Although it has been reviewed by EPA and NOAA and approved for publication, it does not necessarily reflect their policies or views.

References

Acker, K., Moller, D., Wieprecht, W., Meixner, F.X., Bohn, B., Gilge, S., Plass-Dülmer, C., Berresheim, H., 2006. Strong daytime production of OH from HNO_2 at a rural mountain site. Geophysical Research Letters 33, L02809.

Alicke, B., Platt, U., Stutz, J., 2002. Impact of nitrous acid photolysis on the total hydroxyl radical budget during the limitation of oxidant production/Pianura Padana Produzione di Ozono study in Milan. Journal of Geophysical Research 107 (D22), 8196.

Alicke, B., Geyer, A., Hofzumahaus, A., Holland, F., Konrad, S., Pätz, H.W., Schäfer, J., Stutz, J., Volz-Thomas, A., Platt, U., 2003. OH formation by HONO photolysis during the BERLIOZ experiment. Journal of Geophysical Research 108 (D4), 8247.

Ammann, M., Kalberer, M., Jost, D.T., Tobler, L., Rössler, E., Piguet, D., Gäggeler, H.W., Baltensperger, U., 1998. Heterogeneous production of nitrous acid on soot in polluted air masses. Nature 395, 157–160.

Appel, B.R., Winer, A.M., Tokiwa, Y., Biermann, H.W., 1990. Comparison of atmospheric nitrous acid measurements by annular denuder and differential optical absorption systems. Atmospheric Environment 24A, 611–616.

Arens, F., Gutzwiller, L., Baltensperger, U., Gaggeler, H.W., Ammann, M., 2001. Heterogeneous reaction of NO_2 on diesel soot particles. Environmental Science and Technology 35, 2191–2199.

Aumont, B., Chervier, F., Laval., S., 2003. Contribution of HONO sources to the $NO_x/HO_x/O_3$ chemistry in the polluted boundary layer. Atmospheric Environment 37, 487–498.

Bejan, I., Aal, Y.A.E., Barnes, I., Benter, T., Bohn, B., Wiesen, P., Kleffmann, J., 2006. The photolysis of *ortho*-nitrophenols: a new gas phase source of HONO. Physical Chemistry Chemical Physics 8, 2028–2035.

Binkowski, F.S., Roselle, S.J., 2003. Community Multiscale Air Quality (CMAQ) model aerosol component, I: model description. Journal of Geophysical Research 108 (D6), 4183.

Brauer, M., Ryan, P.B., Suh, H.H., Koutrakis, P., Spengler, J.D., Leslie, N.P., Billick, I.H., 1990. Measurements of nitrous acid inside two research houses. Environmental Science and Technology 24, 1521–1527.

Byun, D., Schere, K.L., 2006. Review of the governing equations, computational algorithms, and other components of the models-3: Community Multiscale Air Quality (CMAQ) modeling system. Applied Mechanics Reviews 59, 51–77.

Cai, C., 2005. Implementation and Performance Evaluation of an Air Quality Forecast Modeling System (AQFMS) for Northeastern USA. The University at Albany, State University of New York, New York.

Calvert, J.G., Yarwood, G., Dunker, A.M., 1994. An evaluation of the mechanism of nitrous acid formation in the urban atmosphere. Research on Chemical Intermediates 20, 463–502.

Carter, W.P.L., 2000. Implementation of the SAPRC-99 chemical mechanism into the Models-3: framework. Report to the United States Environmental Protection Agency, available at 〈http://www.cert.ucr.edu/~carter/absts.htm#s99mod3〉.

Dasgupta, P.K., 2007. Personal communication.

Eder, B., Yu, S., 2006. A performance evaluation of the 2004 release of models-3: CMAQ. Atmospheric Environment 40, 4811–4824.

Febo, A., Perrino, C., Cortiello, M., 1993. A denuder technique for the measurement of nitrous acid in urban atmospheres. Atmospheric Environment 27, 1721–1728.

Finlayson-Pitts, B.J., Pitts Jr., J.N., 2000. Chemistry of the Upper Lower Atmosphere, Theory, Experiments and Applications. Academic Press, San Diego.

Gery, M.W., Whitten, G.W., Killus, J.P., Dodge, M.C., 1989. A photochemical kinetics mechanism for urban and regional scale computer modeling. Journal of Geophysical Research 94, 12925–12956.

Gilliam, R.C., Hogrefe, C., Rao, S.T., 2006. New methods for evaluating meteorological models used in air quality applications. Atmospheric Environment 40, 5073–5086.

Grell, G., Dudhia, J., Stauffer, D., 1994. A description of the fifth-generation Penn State/NCAR Mesoscale model (MM5). NCAR Technical Note NCAR/TN-398+STR.

Harris, G.W., Carter, W.P.L., Winer, A.M., Pitts Jr., J.N., Platt, U., Perner, D., 1982. Observation of nitrous acid in the Los

Angeles atmosphere and implications for prediction of ozone precursor relationships. Environmental Science and Technology 16, 414–419.

Harrison, R.M., Peak, J.D., Collins, G.M., 1996. Tropospheric cycle of nitrous acid. Journal of Geophysical Research 101, 14429–14439.

Houyoux, M.R., Vukovich, J.M., Coats Jr., C.J., Wheeler, N.M., Kasibhatla, P.S., 2000. Emission inventory development and processing for the seasonal model for regional air quality (SMRAQ) project. Journal of Geophysical Research 105, 9079–9090.

Jones, M.R., 2006, Ammonia deposition to semi-natural vegetation, Ph.D. Dissertation, University of Dundee, Scotland.

Kessler, C., Platt, U., 1984. Nitrous acid in polluted air masses—sources and formation pathways. In: Versino, B., Angeletti, G. (Eds.), Physico-Chemical Behaviour of Atmospheric Pollutants (Proceedings). Reidel, Dordrecht, pp. 412–422.

Kirchstetter, T.W., Littlejohn, D., 1996. Measurements of nitrous acid in motor vehicle exhaust. Environmental Science and Technology 30, 2843–2849.

Kleffmann, J., Becker, K.H., Wiesen, P., 1998. Heterogeneous NO_2 conversion processes on acid surfaces: possible atmospheric implications. Atmospheric Environment 32, 2721–2729.

Kleffmann, J., Becker, K.H., Lackhoff, M., Wiesen, P., 1999. Heterogeneous conversion of NO_2 on carbonaceous surfaces. Physical Chemistry Chemical Physics 1, 5443–5450.

Kurtenbach, R., Becker, K.H., Gomes, J.A.G., Kleffmann, J., Lorzer, J.C., Spittler, M., Wiesen, P., Ackermann, R., Geyer, A., Platt, U., 2001. Investigations of emissions and heterogeneous formation of HONO in a road traffic tunnel. Atmospheric Environment 35, 3385–3394.

Lammel, G., Perner, D., 1988. The atmospheric aerosol as a source of nitrous acid in polluted atmospheres. Journal of Aerosol Science 19, 1199–1202.

Moussiopoulos, N., Papalexiou, S., Lammel, G., Arvanitis, T., 2000. Simulation of nitrous acid formation taking into account heterogeneous pathways: application to the Milan metropolitan area. Environmental Modelling and Software 15, 629–637.

Perner, D., Platt, U., 1979. Detection of nitrous acid in the atmosphere by differential optical absorption. Geophysical Research Letters 6, 917–920.

Philbrick, C.R., Ryan, W.F., Clark, R.D., Doddridge, B.G., Dickerson, R.R., Koutrakis, P., Allen, G., Munger, J.W., McDow, S.R., Rao, S.T., Hopke, P.K., Eatough, D.J., Dasgupta, P.K., Tollerud, D.J., Georgopoulos, P., Kleinman, L.I., Daum, P., Nunnermacker, L., Dennis, R., Schere, K., McClenny, W., Gaffney, J., Marley, N., Coulter, R., Fast, J., Doren, C., Peter, K., Mueller, P.K., 2002. Overview of the NARSTO-NE-OPS Program, Fourth Conference on Atmospheric Chemistry: Urban, Regional and Global-Scale Impacts of Air Pollutants. American Meteorological Society, Boston, MA, pp. 107–114.

Pitts Jr., J.N., Biermann, H.W., Tuazon, E.C., Green, M., Long, W.D., Winer, A.M., 1989. Time-resolved identification and measurements of indoor air pollutants by spectroscopic techniques: gaseous nitric acid, methanol, formaldehyde, and formic acid. Journal of the Air Pollution and Control Association 39, 1344–1347.

Pleim, J.E., 2007. A combined local and nonlocal closure model for the atmospheric boundary layer. Part I: model description and testing. Journal of Applied Meteorology and Climate 46, 1383–1395.

Simon, P.K., Dasgupta, P.K., 1995. Continuous automated measurement of gaseous nitrous and nitric acids and particulate nitrite and nitrate. Environmental Science and Technology 29, 1534–1541.

Schwede, D., Pouliot, G., Pierce, T., 2005. Changes to the biogenic emissions inventory system version 3 (BEIS3). In: Proceedings of the Fourth Annual CMAS Models-3 Users' Conference, September 26–28, 2005, UNC-Chapel Hill, NC. Available at 〈http://www.cmascenter.org/html/2005_conference/abstracts/2_7.pdf〉.

Svensson, R., Ljungstrom, E., Lindqvist, O., 1987. Kinetics of the reaction between nitrogen dioxide and water vapour. Atmospheric Environment 21, 1529–1539.

Vecera, Z., Dasgupta, P., 1991. Measurements of ambient nitrous acid and a reliable calibration source for gaseous nitrous acid. Environmental Science and Technology 25, 255–260.

Vogel, B., Vogel, H., Kleffmann, J., Kurtenbach, R., 2003. Measured and simulated vertical profiles of nitrous acid—part II, model simulations and indications for a photolytic source. Atmospheric Environment 37, 2957–2966.

Wormhoudt, J., Herndon, S.C., Yelvington, P.E., Miake-Lye, R.C., Wey, C., 2007. Nitrogen oxide (NO/NO_2/HONO) emissions measurements in aircraft exhausts. Journal of Propulsion and Power 23 (5), 906–911.

Winer, A.M., Biermann, H.W., 1994. Long pathlength differential optical absorption spectroscopy (DOAS) measurements of gaseous HONO, NO_2 and HCHO in the California South Coast Air Basin. Research on Chemical Intermediates 20, 423–445.

Yarwood, G., Rao, S., Yocke, M., Whitten, G., 2005. Updates to the Carbon Bond chemical mechanism: CB05. Final report to the US EPA, RT-0400675, available at 〈http://www.camx.com/publ/pdfs/CB05_Final_Report_120805.pdf〉.

Zhou, X., Beine, H.J., Honrath, R.E., Fuentes, J.D., Simpson, W., Shepson, P.B., Bottenheim, J.W., 2001. Snowpack photochemical production of HONO: a major source of OH in the arctic boundary layer in springtime. Geophysical Research Letters 28, 4087–4090.

Zhou, X., Civerolo, K., Dai, H., Huang, G., Schwab, J.J., Demerjian, K.L., 2002. Summertime nitrous acid chemistry in the atmospheric boundary layer at a rural site in New York State. Journal of Geophysical Research 107 (D21), 4590.

Zhou, X., Gao, H., He, Y., Huang, G., Bertman, S.B., Civerolo, K., Schwab, J., 2003. Nitric acid photolysis on surfaces in low-NO_x environments: significant atmospheric implications. Geophysical Research Letters 30 (23), 2217.